AD-A052 884 DAVID W TAYLOR NAVAL SHIP RESEARCH AND DEVELOPMENT CE--ETC F/G 20/4
UNSTEADY CAVITATION ON AN OSCILLATING HYDROFOIL.(U)
JAN 78 Y T SHEN, F B PETERSON

UNCLASSIFIED 78-SPD-809-01 NL

1 OF 1
AD
A052884

END
DATE
FILMED
5-78
DDC

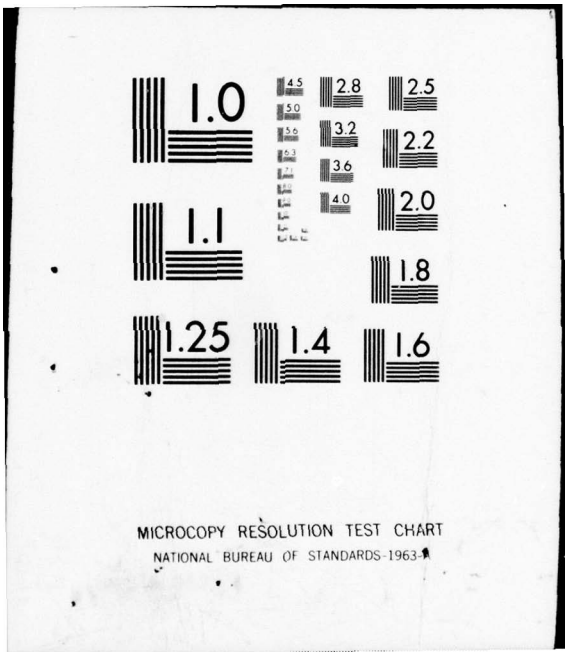
1.0
1.1
1.25
1.4
1.6
1.8
2.0
2.2
2.5
2.8
3.2
3.6
4.0
4.5
5.0
5.6
6.3
MICROCOPY RESOLUTION TEST CHART
NATIONAL BUREAU OF STANDARDS-1963-A

DAVID W. TAYLOR NAVAL SHIP RESEARCH AND DEVELOPMENT CENTER

Bethesda, Md. 20084

UNSTEADY CAVITATION ON AN OSCILLATING HYDROFOIL

by

Young T. Shen and
Frank B. Peterson

APPROVED FOR PUBLIC RELEASE: DISTRIBUTION UNLIMITED

SHIP PERFORMANCE DEPARTMENT
DEPARTMENTAL REPORT

January 1978

78-SPD-809-01

MAJOR DTNSRDC ORGANIZATIONAL COMPONENTS

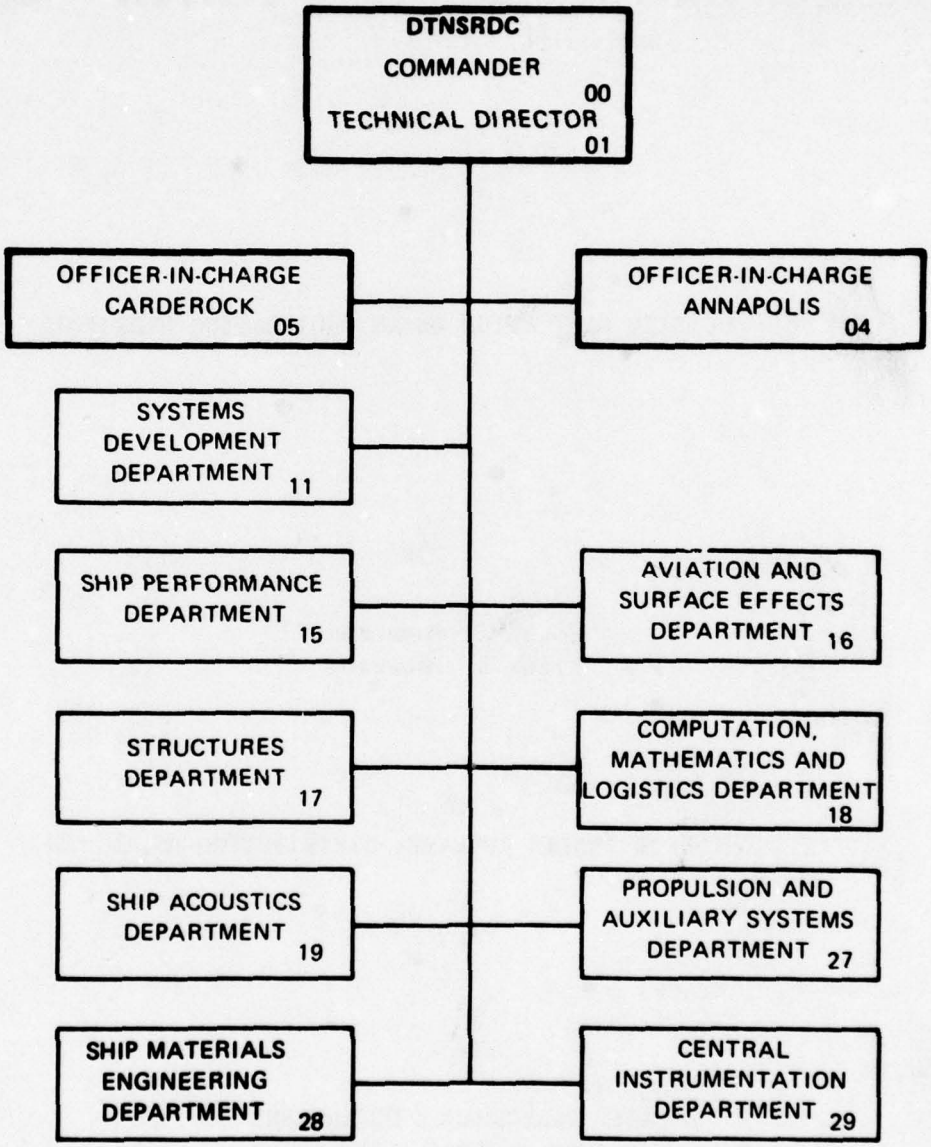

UNCLASSIFIED

SECURITY CLASSIFICATION OF THIS PAGE (When Data Entered)

REPORT DOCUMENTATION PAGE

READ INSTRUCTIONS BEFORE COMPLETING FORM

1. REPORT NUMBER: 78-SPD-809-01	2. GOVT ACCESSION NO.	3. RECIPIENT'S CATALOG NUMBER
4. TITLE (and Subtitle): Unsteady Cavitation on an Oscillating Hydrofoil		5. TYPE OF REPORT & PERIOD COVERED: Research and Development rept.
		6. PERFORMING ORG. REPORT NUMBER
7. AUTHOR(s): Young T. Shen and Frank B. Peterson		8. CONTRACT OR GRANT NUMBER(s)
9. PERFORMING ORGANIZATION NAME AND ADDRESS: David W. Taylor Naval Ship R&D Center, Bethesda, MD 20084		10. PROGRAM ELEMENT, PROJECT, TASK AREA & WORK UNIT NUMBERS: Task Area SF43452703 Element 62543N (Task Area GHR Element 61153N SR0230101)
11. CONTROLLING OFFICE NAME AND ADDRESS: Naval Sea Systems Command, Washington, D.C. 20350		12. REPORT DATE: Jan 78
		13. NUMBER OF PAGES: 36 (12) 41p.
14. MONITORING AGENCY NAME & ADDRESS (if different from Controlling Office): (16) F43452, SR0230701 (17) SF4345270 3, SR0230101		15. SECURITY CLASS. (of this report): Unclassified
		15a. DECLASSIFICATION/DOWNGRADING SCHEDULE

16. DISTRIBUTION STATEMENT (of this Report)

APPROVED FOR PUBLIC RELEASE: DISTRIBUTION UNLIMITED

17. DISTRIBUTION STATEMENT (of the abstract entered in Block 20, if different from Report)

18. SUPPLEMENTARY NOTES

19. KEY WORDS (Continue on reverse side if necessary and identify by block number)

Cloud Cavitation; Oscillating Hydrofoil; Propellers

20. ABSTRACT (Continue on reverse side if necessary and identify by block number)

Bent trailing edges and erosion which are often observed on marine propellers, are attributed mainly to unsteady cavitation caused by the non-uniformity of flow field behind ship's hull. In order to improve the physical understanding, the formation of cloud cavitation and bubble collapse on marine propellers, a two-dimensional hydrofoil was tested at the DTNSRDC 36-inch water tunnel under pitching oscillation. The inception of cavitation, cavity growth and collapse were investigated in terms of the reduced → cont

DD FORM 1 JAN 73 1473 EDITION OF 1 NOV 65 IS OBSOLETE S/N 0102-014-6601

389 694 JOB

UNCLASSIFIED

SECURITY CLASSIFICATION OF THIS PAGE (When Data Entered)

Cont.

UNCLASSIFIED

frequency. The possible cause of "cloud cavitation" and the applicability of a quasi-steady method to predict unsteady cavitation were investigated and discussed.

UNCLASSIFIED

TABLE OF CONTENTS

ABSTRACT

Bent trailing edges and erosion,which are often observed on marine propellers,are attributed mainly to unsteady cavitation caused by the non-uniformity of flow field behind ship's hull. In order to improve the physical understanding, the formation of cloud cavitation and bubble collapse on marine propellers, a two-dimensional hydrofoil was tested at the DTNSRDC 36-inch water tunnel under pitching oscillation. The inception of cavitation, cavity growth and collapse were investigated in terms of the reduced frequency. The possible cause of "cloud cavitation" and the applicability of a quasi-steady method to predict unsteady cavitation were investigated and discussed.

ADMINISTRATIVE INFORMATION

The work described in this report is sponsored by Naval Sea Systems Command Code 037 under Element 62543N, Task Area SF43452703, and partly supported under the General Hydrodynamic Research Program, Element 61153N, Task Area SR0230101. Work Unit Number 1-1552-817-01.

INTRODUCTION

It has been well observed that for a nominally steady sheet cavity there are relatively few collapsing vapor bubbles to produce the erosion.[1] However, if a propeller blade enters the high wake field, sheet cavitation starts from the leading edge, passes the region of maximum wake defect and cavity is separated and thickened, while leaving the high wake zone it collapses and under certain conditions becomes cloudy. This type of cavitation is called cloud cavitation and is considered to be the main cause of the erosion, and bent trailing edges.[2]

Model experiments have been performed by many organizations in an attempt to simulate the full scale wake fields in which a propeller operates. A recent discussion on this subject was given by Tanibayashi[2]. An experimental study to determine the importance of unsteady propeller cavitation on induced hull pressure was performed by Chiba and Hoshino.[3] Ito[4] performed experimental investigations concerned with unsteady cavitation on propellers in a wake field by oscillating a three-dimensional wing.

To improve the physical understanding on formation of cloud cavitation and bubble collapse of marine propellers, a two-dimensional oscillating hydrofoil was studied by Tanibayasi and Chiba,[5] and later by Miyata et al.[6] Their experiments (Reference 5) showed that the behavior of the cavities just before collapse was quite similar to cloud cavitation which was observed in propeller cavitation tests in nonuniform flow.

A two-dimensional oscillating foil is seen to produce useful data in terms of cavity dynamics such as inception,growth and collapse.

In Reference 7, Huang and Peterson showed that the viscous effect played a significant role in the cavitation-inception study at model scale. In order to simulate the viscous effect as close to a prototype as possible, the Reynolds number used in the model should be as high as possible. This situation could be tested (to some extent) by using a relatively large scale model in a 36-inch water tunnel with high tunnel speeds.

The objectives of the present study were to investigate the mechanisms of cavitation-inception, cavity growth and collapse. In view of complicated flow patterns on a marine propeller, these problems could best be studied with a two-dimensional oscillating hydrofoil at high Reynolds numbers.

APPARATUS AND TEST PROCEDURE

MODEL SIZE

A rectangular wing was used in this test. The wing section is a Joukowski profile with a trailing edge modified to eliminate the cusp. It is 10.5 percent thickness-to-chord ratio. The chord length is 241 mm and the span is 823 mm. The model is made of stainless steel. The foil surface was hand finished within 38 μ-cm RMS.

Four pressure gage transducers were installed at 5.3 , 7.87, 24.1, and 60.3 mm from the leading edge. These give the locations of pressure gages at 2.2, 3.3 , 10, and 25 percent chord from the leading edge. They are recess type pressure gages designed to measure the unsteady pressure distribution due to foil oscillation and boundary layer pressure fluctuation measurements. The foil was also instrumented with dye observation and lift measurement.

APPARATUS

The oscillating foil was tested at the DTNSRDC 36-inch water tunnel. The circular cross section was converted into an approximately two-dimensional test section by two pieces of liners installed on each side of the wall as shown in Figure 1. The foil was pitched around the quarter chord from the leading edge. The apparatus around the test section is shown in Figure 2.

TEST PROCEDURE

The objective of the present study was to investigate the unsteadiness effect on cavity dynamics. The air content was measured with 70% saturation in reference to atmospheric pressure at water temperature of 72°F and tunnel pressure of 103.6 KPa. Then the hydrodynamic characteristics of an oscillating foil in terms of cavitation can be described by the following non-dimensional parameters: Reynolds number (Re), reduced frequency (K) and vapor cavitation number (σ_v).

In order to simulate the viscous effect as close to the prototype as possible, tunnel speeds of 9.85 to 16.43 m/sec. were used in the tests. The corresponding Reynolds numbers of 2.44×10^6 to 4.01×10^6 were achieved at 70°F water temperature. They are an order of magnitude higher than the values achieved in References 5 and 6.

The range of reduced frequency at 0.7 radius of a typical marine propeller can be approximated by

$$K = \frac{\omega c}{2\sqrt{V_A^2 + (0.7\,\omega R)^2}}$$

$$\sim \frac{c}{1.4R} \qquad \text{for } V_A \ll 0.7\,\omega R$$

$$\sim 0.3 \text{ to } 0.8$$

The oscillating frequencies of 4 Hz to 25 Hz were selected to cover the desired range of reduced frequency.

The study of cavity dynamics was based on flow observation. In every test condition, 25 pictures were taken to record the cavity formation on the foil. A pulse signal was simultaneously recorded in the magnetic tape when a picture was taken. In this way, each cavity pattern observed on the foil could be related directly to the instantaneous angle of attack on the foil. The picture size only covered approximately one third of the foil span.

INCEPTION OF CAVITATION

In order to simulate the viscous effect as close to a prototype as possible, the model was tested at high tunnel speeds. For a given body shape the non-dimensional laminar boundary layer thickness based on the chord decreases as $1/\sqrt{Re}$. The hydrodynamic roughness of the surface becomes less smooth at higher Reynolds number. This hydrodynamic characteristic was reflected in the present model tests with cavitation inception triggered prematurely by two "weak" spots near the geometric leading edge around the midspan , where the pictures were taken. Many attempts had been tried to smooth the foil surface to eliminate the " spots without success. As to be seen in the subsequent discussion, the difference between cavitation inception and desinent cavitation is small for sheet cavitation. The effect of these two "weak" spots on desinent cavitation was found to be negligible. Consequently, the tests were continued.

A steady-flow condition corresponds to a limiting case of an oscillating hydrofoil with zero frequency. Consider the case of a hydrofoil tested in a uniform stream of 11.49 m/sec. The angle of attack was set at 3.5 degrees without oscillation. The ambient pressure at the test section was gradually reduced from an initially high static pressure. The cavitation patterns on the foil at P_{amb} = 76.6 and 76.3 KPa were sketched in Figures 3a and 3b, where "spot type" cavitation are visible. Many attempts were conducted to eliminate these "weak" spots without success. However, it is noted that a small reduction in ambient pressure from 76.6 to 76.3 KPa produced a leading edge sheet cavity. It is believed that this condition

would closely represent cavitation-inception if the foil surface were free of these two "weak" spots.

This flow observation will now be compared with a theoretical prediction. The minimum pressure envelope of this foil obtained from the Brockett program[8] (see Figure 4A) is obtained from the potential flow theory with lift slope coefficient of 2π. In a real fluid the minimum pressure envelope will be modified slightly. The measured inception angles were slightly higher than the values predicted theoretically. Nevertheless, the agreement between flow observation and theoretical prediction is quite reasonable. The location of $-C_{pmin}$ versus angle of attack computed theoretically is given in Figure 4B. Experimental observation indicated that the leading edges of sheet cavities were located approximately from 0.01C to 0.035C, where C is the chord length. The exact location depends on which sheet cavity was referred. The foil was designed to have laminar boundary layer separation free at α = 3.5 deg. and velocity V_∞ = 10.27 m/sec. This design consideration was verified in experiments as seen in Figure 4B.

Next, we fixed the ambient pressure at P_{amb} = 76.3 KPa, and the velocity at V_∞ = 11.49 m/sec. Then, the foil angle was gradually reduced. At α = 3.35°, the flow pattern on the foil regained a similar appearance to that given in Figure 3a, where cavities due to "weak" spots remained visible. Nevertheless, this condition should represent desinence cavitation had the foil surface been absent of "weak" spots. Similar results was observed with tunnel speed of 16.43 m/s and an ambient pressure of 165.7 KPa. These data are plotted in Figure 4A.

Because of the presence of "weak" spots the inception of cavitation is not easy to define precisely. On the other hand, as described in the subsequent discussion on the oscillating foil, the desinence cavitation can be identified more precisely without difficulty. In view of the relatively small difference between inception and desinence, the cavitation study will be given under the title of desinent cavitation.

UNSTEADY EFFECTS ON CAVITY GROWTH AND COLLAPSE

The foil was oscillated sinusoidally around the quarter chord from the leading edge. Then, the hydrodynamic characteristics of an oscillating foil in terms of cavitation were described by the following nondimensional parameters, Re, K, and σ_v. The instantaneous foil angle of attack α is given by

$$\alpha = \alpha_o + \bar{\alpha} \sin(\omega t)$$

where α_o, $\bar{\alpha}$, ω and t are mean angle, pitch amplitude, pitch frequency and time respectively.

The major test matrix carried out for cavity dynamic studies is given in Table 1. The ranges of major nondimensional parameters tested were Re = 2.44×10^6 to 4.01×10^6, σ_v = 1.11 to 1.309, and K = 0.2 to 1.65. The range of reduced frequency was chosen to cover the domain of practical interest in propeller applications.

The study of cavity dynamics was based on flow observation. Twenty-five pictures were taken of each test condition. A picture was taken every ten oscillations plus 1/25 the foil period of the foil. Thus, a series of high quantity, short duration photos were taken that together simulated one complete cycle of the foil oscillation. Because of good sinusoidal motion, the cavity formation observed in the subsequent pictures is very systematic. A typical historical diagram of angle-of-attack oscillation is shown in Figure 5. On top of the figure is the signal from the pulse channel

which recorded that instant of time when the picture was taken. In this way, each cavity pattern observed on the picture could be related uniquely to the instantaneous angle of incidence on the foil. It is remarked that the foil span is 823 mm and the picture was taken around the mid-span with a picture width of approximately 254 mm.

As mentioned in the "Introduction", the breaking of the sheet cavity generates many smaller cavities. If these many small vapor bubbles are generated in a region of pressure greater than the vapor pressure, their collapse will be extremely rapid. The collapse of each individual small vapor bubble may be responsible for the erosion. Therefore, the major attention in this study is focused on the subject of cavity breaking and the formation of cloud cavities.

Two series of test runs will be given to provide a contrast on the degree of cavity breaking. The sequential pictures taken from the test run of the 1301 series along with the instantaneous angle of attack are given in Figure 6. The incoming flow velocity and ambient pressure were V_∞ = 11.49 m/s and P_{amb} = 76.3 KPa. At 70°F water temperature, this setup gave Re = 2.84 x 10^6 and σ_v = 1.117, respectively. The foil mean angle of attack was set at 3 degrees. The foil was oscillated at 4.0 Hz (K=0.26) with a pitch amplitude of 1 degree. At Figures 6d, and 6e, reentrant jets formed at the rear end of cavities, gradually filling them with foam and causing a vortex type motion within the cavities. The maximum cavity length as measured from the foil leading edge is approximately 0.30C with C the

chord length. From Figures 6h to 6i, the cavities disappear distinctly from the foil surface except at two "weak" spots. The condition at Figure 6i will be referred as desinence cavitation of the oscillating foil.

Sequential pictures taken from the test run of series 1401 with a pitch amplitude of 1.5 degrees are given in Figure 7. It is noted that the only difference between 1301 and 1401 series were the magnitude of the pitch amplitude. Strong reentrant jet mixing is again seen in Figures 7d and 7e. However, they were then followed by a sequence of violent cavity breaking and the formation of cloud cavitation. The maximum cavity length is approximately 0.4C.

Even in a nominally steady sheet cavity a partial cavity flow exhibits a strong property of unsteadiness. Experiments carried out by Wade and Acosta[9] show that this unsteady region persisted over a region of cavity length to chord length ratios of approximately 0.6 to 1.2. On either side of this region the flow was relatively steady. However, the test results obtained from the present oscillating foil suggested that the cavity was relatively smooth if the cavity length was less than 0.35. The cavity length was gradually shortened and disappeared smoothly as the foil angles were gradually decreased. On the other hand, strong breakup of sheet cavity started to appear when the cavity length reached 0.4C. The degree of breakup became stronger as the length of cavity was further increased, for example by reducing the cavitation number. Thus the characteristics of unsteady partial cavity flow were seen to follow the same pattern as that of a steady one, except, the appearance of unsteadiness took place earlier

at smaller cavity length.

The reduced frequency, K, can be expressed as follows:

$$K = \frac{\omega c}{2U} = \pi \frac{c}{\lambda}$$

where λ is the wave length of disturbance. Therefore, the degree of unsteadiness can be studied in terms of K. The effect of reduced frequency on cavity dynamics will now be examined. In Series 1401, the foil was oscillated at 4.0 Hz with reduced frequency of K = 0.26. A sequence of pictures for Series 1403 were taken (see Figure 8) with foil oscillated at 7.5 Hz corresponding to a reduced frequency of K = 0.49.

The maximum cavity length remained approximately around 0.4C. Once again strong breakup in sheet cavity is visible in the Figures 8e and 8f. A comparison of Figures 7 and 8 show that as expected, the development of cavities was delayed in Series 1403 than in Series 1401. In addition, the formation of cloud cavities was stronger in the 1403 series. As seen in Figures 8k and 8l, cloud cavities were still visible on the foil long after the leading edge sheet cavities disappeared.

A cloud of vapor and/or many small cavities are generated when the sheet cavity breaks up. These small cavities are transported approximately at the free stream speed. For the cases of Series 1401 and 1403, due to the phase shift in unsteady flow the sheet cavity breaks up at the angle of attack slightly behind the maximum angle. As the bubbles or small cavities are transported downstream, the oscillation of the foil angles simultaneously decreases. The magnitude of the suction pressure is greatly

reduced that is, the bubbles (small cavities) enter a higher pressure region with the foil in oscillation rather than steady. The cloud of vapor and/or small cavities seem to undergo a process of condensation. This may provide an environment for cloud cavitation to form. The formation of cloud cavitation was thus more visible in the 1403 series than in the 1401 series. On the other hand, further increase in reduced frequency above k = 0.5 resulted in a decrease in cavity size. Consequently, the strongest breaking of sheet cavity was seen to attain a maximum from k = 0.4 to 0.5. This phenomenon was observed throughout the whole series of tests as indicated in Table 1.

The study of cavity dynamics in a water tunnel also encounters a fundamental question, namely, the effect of tunnel compliance and its effect on such transient cavity flows. For example, if the tunnel were perfectly rigid and if there were no free surfaces other than that of cavity itself, then an infinite pressure difference in an incompressible medium would be required to create the changing cavity volume. To make sure that this kind of tunnel effect would not be present in our model tests, a hydraulically-operated piston over a frequency range of 0 to 45 Hz was plunged into the 36-inch water tunnel sinusoidally to simulate the possible maximum changing cavity volume. A sharp peak of fundamental tunnel resonance was observed at 4.7 Hz. Consequently, all the oscillating studies had been carried out at frequencies away from that resonant frequency.

Experimental investigations concerned with unsteady cavitation on a propeller in a wake field were performed by Ito[4]. One of his principal results was that there exists a critical reduced frequency at which a leading edge sheet cavity breaks up producing cloud cavitation at approximately k = 0.3 to 0.4.

On the other hand Tanibayashi and Chiba[5] did not demonstrate the existence of a critical reduced frequency as did the work of Ito[4]. The cavitation occurred in the experiments of Tanibayashi and Chiba and was in the form of travelling bubbles. In the present work all the cavitation occurred as sheet cavitation. Strong breakup of sheet cavitation and the formation of cloud cavitation were observed around the reduced frequency of K = 0.4 to 0.5, similar to that first reported by Ito.

It was observed in the present study that the growth and collapse of the sheet cavity in the oscillating foil followed the same trend of cavity dynamics as a steady foil with cavity lengths between 0.6C and 1.2C. A linearized theory of unsteady partial cavity flow was developed by Steinberg and Karp.[10] However, it is noted that the breakup of sheet cavity is a nonlinear phenomenon. If this physical phenomenon is to be simulated mathematically, a theory of full nonlinear unsteady partial cavity flow must be developed.

The possibility of using a quasi-steady concept in cavity dynamics will now be discussed. The instantaneous angles of attack of Figures 6a and 6g are approximately the same. However, completely different cavitation patterns are observed. The same conclusion is also applicable to Figures 7a and 7g. Within the range of reduced frequency of interest in marine propellers, the application of the quasi-steady assumption in partial cavity dynamics does not appear to be valid.

DESINENT CAVITATION

In a steady flow desinent cavitation can be uniquely defined. In an unsteady cavity flow of large cavity length, two types of desinent cavitation were observed. The first type is related to leading edge sheet cavitation and the second type corresponds to bubble cavitation. As seen in Figures 7j and 7k, the surface sheet cavity disappeared at Figure 7k; however, cloud cavitation is still visible in Figure 7k, being referred to as surface desinent cavitation. Similarily, when cloud cavitation is not visible on the foil, that condition is referred to as cloud desinent cavitation.

At conditions of cavitation-inception and desinent cavitation, the size of the cavity with respect to the cloud on the foil is extremely small. Thus, wing theories are expected to predict the proper flow field. A simple example is the classic Theoderson wing theory of a flat plate with small oscillation.[11] The lift slope coefficients and pitch phase angles with respect to the quarter chord from the leading edge are given in Figure 9. A minimum of foil lift around the reduced frequency of 0.3 to 0.5 is observed. Recently, experiments with two-dimensional pitching hydrofoils of various NACA sections were performed by Radhi.[12] Based on the inception curves presented it appears that inception was suppressed as the reduced frequency approached nominal values from 0.4 to 0.5. This phenomenon was also observed in the work of Miyata et al.[6] The extent to which these experimental results can be correlated with the minimum in total lift still must be determined.

Only 25 pictures were taken to cover one cycle of oscillating motion, and thus the angle at which desinence occurred can only be related to two successive pictures. Therefore, the desinent angle is given in terms of a small range of angles instead of a single value. For example, the desinent angle on Series 1301 is α_{des} = 3.05 ~ 3.29 deg. The unsteady effect on desinent cavitation is given in Table 2 and Figure 10. Qualitatively, the surface desinent cavitation follows the same trend as the work of Miyata et al and the inception measurements of Radhi. The lack of a peak at k = 0.4 to 0.5 in the present desinent cavitation study may be due partly to the lack of sharp resolution in angle measurement.

The cavity effect on desinent cavitation will now be discussed. For the same values of Re and σ_v , the desinent cavitation of the 1301 series with pitch amplitude of 1.0 degree, and the 1401 series with pitch amplitude of 1.5 degrees are given in Figure 11. The surface cavitation desinent angles of the 1401 series were systematically lower than those of the 1301 series at the same reduced frequency. Physically, this nonlinear effect on desinent cavitation may be related to a so-called "pressure gradient" effect. However, the correlation with unsteady pressure distribution still must be accomplished. The 1205 series (Table 2c) had a pitch amplitude of 2.5 degrees. Unfortunately, a direct comparison of this series with the previous two series was not possible because of a significant difference in cavitation numbers.

The classic wing theories assuming flat plate and small oscillation suffer a critical drawback for the cavitation-inception study. The theories give a singularity at the leading edge with infinite velocity and pressure. This type of unrealistic pressure distribution was modified by Miyata et al with the use of experimental data obtained at the K = 0 condition. They were able to obtain reasonable agreement between experimental measurements and the modified theoretical prediction.

All of the surface desinent cavitation information obtained in the present study are relatively consistent (see Table 2). References 6 and 13 along with the present study seem to suggest that desinent cavitation of an oscillating foil might be predicted reasonably well by wing theories if the nonlinear effects such as pressure gradient and exact foil profile are correctly incorporated.

SUMMARY AND CONCLUSION

A two-dimensional hydrofoil was tested at the DTNSRDC 36-inch water tunnel under pitching oscillation. In order to simulate the viscous effect as close to the prototype as possible, the model was tested at high tunnel speeds. The undesirable laminar boundary layer separation on the foil was successfully avoided with the test conditions.

At the steady flow condition, the measured inception of cavitation agrees reasonably well with the theoretical prediction. The difference in angles between cavitation-inception and desinence was found to be small.

Two types of desinent cavitation, surface and cloud, were observed on the oscillating foil. Qualitatively, the surface desinent cavitation as shown in Figure 11 follows the same trend as the works of Miyata and Radhi. In addition, Figure 12 indicates that the surface desinent cavitation is affected by the magnitude of pitch amplitude or pressure gradient.

The present study along with the works given in References 6 and 13, suggest that surface desinent cavitation of an oscillating foil might be predicted reasonably well by wing theories if the nonlinear effect such as pressure gradient and exact foil profile are correctly incorporated.

Without further development in unsteady cavity flow theories, cloud desinent cavitation can only be predicted by model testing. The application of the quasi-steady method will not give a reasonable prediction in terms of cloud desinent cavitation.

The characteristics of unsteady partial cavity flow such as cavity growth, breaking, and formation of cloud cavitation follows the same pattern as that of a steady one, except, the appearance of unsteadiness occurred earlier at a smaller cavity length. The degree of cavity breakup becomes stronger as the length of the cavity is increased.

As the sheet cavity breaks up into many small cavities, they enter a higher pressure region with the foil oscillating rather than steady. This high pressure region in unsteady flow provides an environment for cloud cavitation to form.

The degree of cavity breakup and the formation of cloud cavitation reaches a maximum around the reduced frequency of 0.4 to 0.5, as first reported by Ito.

Within the range of the reduced frequency, of interest in marine propellers, the application of the quasi-steady assumption of cavitation patterns in partial cavity dynamics does not appear to be valid.

The foil was instrumented with pressure gages for pressure distribution studies and strain gages for lift measurements. The test data were recorded on magnetic tapes. Further studies of the data should provide quantitative information supporting the previous conclusion.

ACKNOWLEDGMENT

Grateful appreciation is expressed to Mr. G. Kuiper for his helpful discussions and preparation of the test set-up.

REFERENCES

1. "Unsteady Blade Surface Cavitation" by International Towing Tank Conference Cavitation Committee Report," Tokyo, Japan (1977).

2. Tanibayashi, H., "Practical Approach to Unsteady Problems of Propellers," International Shipbuilding Progress, Vol. 20, No. 226 (1973).

3. Chiba, N. and T. Hoshino, "Effect of Unsteady Cavity on Propeller Induced Hydrodynamic Pressure," Journal of the Society of Naval Architects of Japan, Vol. 139 (1976).

4. Ito, T., "An Experimental Investigation into the Unsteady Cavitation of Marine Propellers," Proceedings of IAHR - Symposium on Cavitation and Hydraulic Machinery, Sendai, Japan (1962).

5. Tanibayashi, H. and N. Chiba, "Unsteady Cavitation of Oscillating Hydrofoil," Mitsubishi Heavy Industries Technical Report (in Japanese), Vol. 5, No. 2 (1968).

6. Miyata, H. et al., "Pressure Characteristics and Cavitation on an Oscillating Hydrofoil," Journal of the Society of Naval Architects of Japan, Vol. 132, No. 10 (1972).

7. Huang, T. and F. Peterson, "Influence of Viscous Effects on Model/ Full Scale Cavitation Scaling," Journal of Ship Research Vol. 20 (1976).

8. Brockett, T., "Steady Two-Dimensional Pressure Distributions on Arbitrary Profiles," DTMB Report 1821 (Oct 1965).

9. Wade, R.B. and A.J. Acosta, "Experimental Observations on the Flow Past a Plano-Convex Hydrofoil," ASME, Journal of Basic Engineering, Vol. 88, No. 1 (1966).

10. Steinberg, H. and S. Karp, "Unsteady Flow Past Partially Cavitated Hydrofoils," Fourth Symposium on Naval Hydrodynamics, Office of Naval Research (1962).

11. Langan, T.J. and D.W. Coder, "Calculated Hydrodynamic Loads on an Oscillating Hydrofoil," DTMB Report 1695 (1965).

12. Radhi, M.N., "Theoretische und Experimentelle Untersuchung uber den Kavitatiouseinsatz au Schwingeuden Tragflugelprofilen," Ph.D Thesis, Technischen Universitat Berlin, D83 (1975).

TABLE 1 - TEST MATRIX OF OSCILLATING FOIL

Run No.	Vel M/S	$Re \times 10^{-6}$	ω Hz	K	P_{amb} KPa*	σ_v	$\bar{\alpha}$ deg
1205	9.85	2.44	4	.31	66.0	1.31	2.5
1206		2.44	5.5	.42		1.31	2.5
1207		2.44	7.5	.58		1.31	2.5
1208		2.44	10.0	.77		1.31	2.5
1301	11.49	2.84	4	.26	76.3	1.12	1.0
1302		2.84	5.5	.36		1.12	1.0
1303		2.84	7.5	.49		1.12	1.0
1304		2.84	10.0	.66		1.12	1.0
1305		2.84	15.0	.99		1.12	1.0
1306		2.84	25.0	1.65		1.12	1.0
1307	14.78	3.66	4	.21	124.3	1.11	1.0
1308		3.66	5.5	.28		1.11	1.0
1309		3.66	7.5	.38		1.11	1.0
1310		3.66	10.0	.51		1.11	1.0
1401	11.49	2.84	4	.26	76.3	1.12	1.5
1402		2.84	5.5	.36		1.12	1.5
1403		2.84	7.5	.49		1.12	1.5
1404		2.84	10.0	.66		1.12	1.5
1405		2.84	15.0	.99		1.12	1.5
1406		2.84	25.0	1.65		1.12	1.5
1407	14.78	3.66	4	.21	127.7	1.15	1.5
1408		3.66	5.5	.28		1.15	1.5
1409		3.66	7.5	.38		1.15	1.5
1410		3.66	10.0	.51		1.15	1.5
1501	16.42	4.01	4	.18	158.8	1.15	1.0
1502		4.01	5.5	.25		1.15	1.0
1503		4.01	7.5	.35		1.15	1.0
1504		4.01	10.0	.46		1.15	1.0
1505		4.01	15.0	.69		1.15	1.0
1506		4.01	25.0	1.15		1.15	1.0

*1 PSI = 6.905 KPa

TABLE 2 - DESINENT CAVITATION

(A) $\bar{\alpha}$ = 1.0 deg

Run No.	$Re \times 10^{-6}$	K	σ_v	Surface α des	Surface α des
1301	2.84	.26	1.12	3.05 ~ 3.29	No
1302	2.84	.36	1.12	3.05 ~ 3.29	No
1303	2.84	.49	1.12	3.05 ~ 3.29	No
1304	2.84	.66	1.12	3.05 ~ 3.29	No
1305	2.84	.99	1.12	2.80 ~ 3.05	2.56 ~ 2.80
1306	2.84	1.65	1.12	2.35 ~ 2.56	2.01 ~ 2.06
1307	3.66	.21	1.11	3.05 ~ 3.29	No
1308	3.66	.28	1.11	3.05 ~ 3.29	No
1309	3.66	.38	1.11	3.05 ~ 3.29	2.80 ~ 3.05
1310	3.66	.51	1.11	3.05 ~ 3.29	2.35 ~ 2.56
1501	4.01	.18	1.15	3.05 ~ 3.29	No
1502	4.01	.25	1.15	3.05 ~ 3.29	No
1503	4.01	.35	1.15	3.05 ~ 3.29	2.80 ~ 3.05
1504	4.01	.46	1.15	2.80 ~ 3.05	2.35 ~ 2.56
1505	4.01	.69	1.15	2.80 ~ 3.05	2.56 ~ 2.80
1506	4.01	1.15	1.15	2.56 ~ 2.80	2.18 ~ 2.35

TABLE 2 - DESINENT CAVITATION

(B) $\bar{\alpha}$ = 1.5 deg

Run No.	Re_{-6} x 10^{-6}	K	σ_v	Surface α_{des}	Bubble α_{des}
1401	2.84	.26	1.12	2.69 ~ 3.07	2.34 ~ 2.69
1402	2.84	.36	1.12	2.69 ~ 3.07	2.03 ~ 2.34
1403	2.84	.49	1.12	2.69 ~ 3.07	1.77 ~ 2.03
1404	2.84	.66	1.12	2.69 ~ 3.07	1.51 ~ 1.60
1405	2.84	.99	1.12	2.34 ~ 2.69	1.62 ~ 1.80
1406	2.84	1.65	1.12	1.77 ~ 2.03	All Frames
1407	3.66	.21	1.16	2.69 ~ 3.07	2.34 ~ 2.69
1408	3.66	.28	1.16	2.69 ~ 3.07	2.34 ~ 2.69
1409	3.66	.38	1.16	2.69 ~ 3.07	1.77 ~ 2.03
1410	3.66	.51	1.16	2.69 ~ 3.07	2.03 ~ 2.34

(C) $\bar{\alpha}$ = 2.5 deg

1205	2.44	.31	1.31	3.12 ~ 3.73	1.38 ~ 1.90
1206	2.44	.42	1.31	3.73 ~ 4.30	1.90 ~ 2.49
1207	2.44	.58	1.31	3.12 ~ 3.73	1.38 ~ 1.90
1208	2.44	.77	1.31	3.12 ~ 3.73	.66 ~ .95

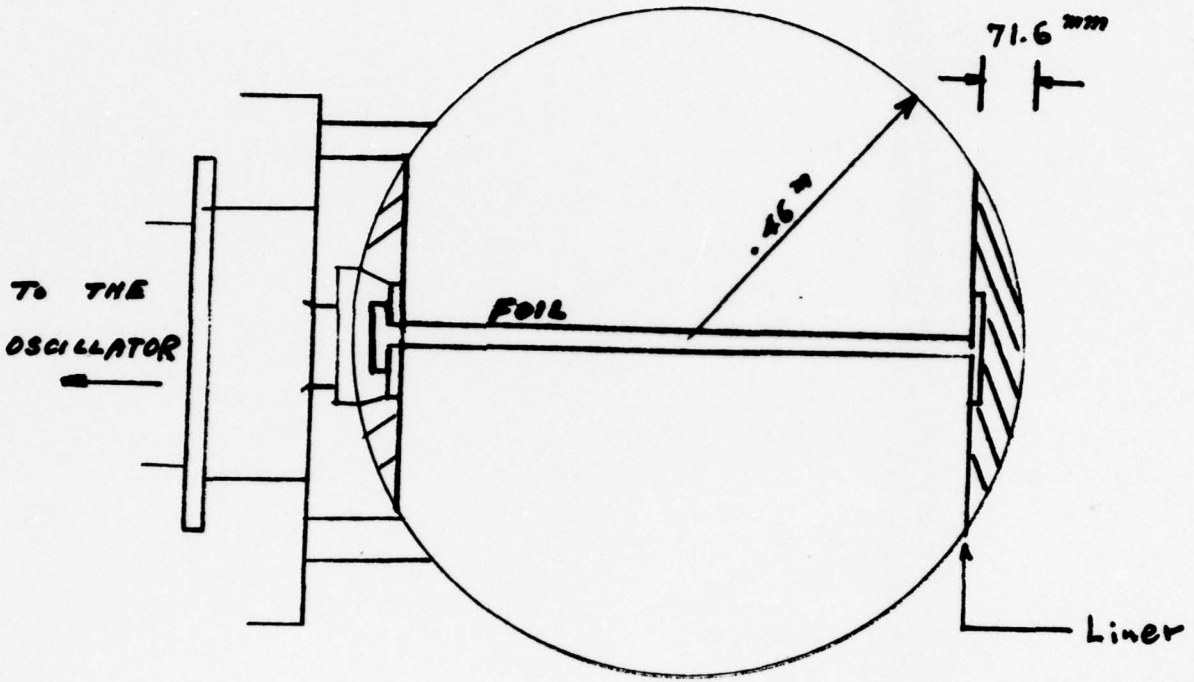

Figure 1 - 36-Inch Water Tunnel With Liners

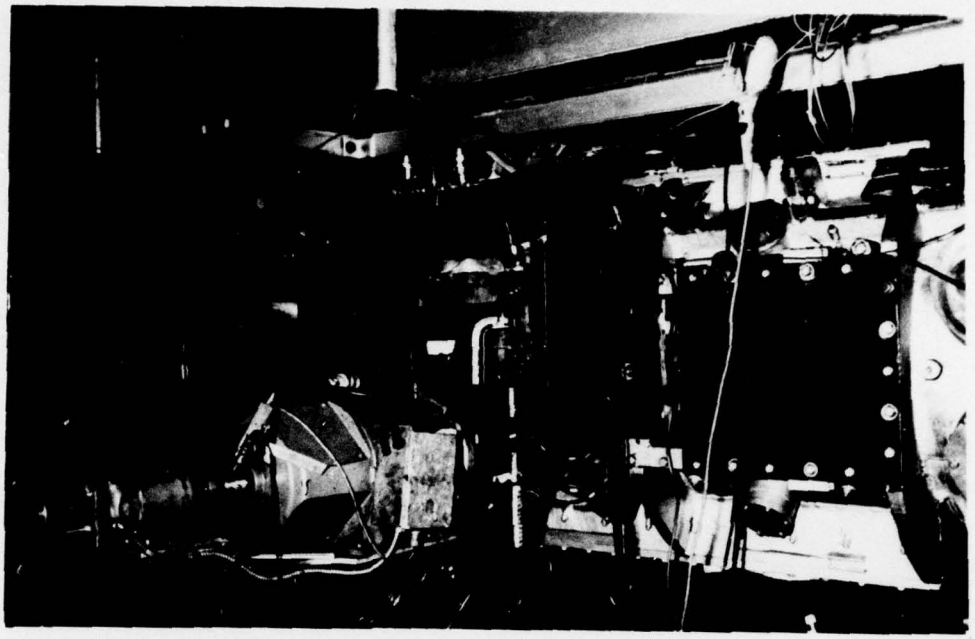

Figure 2 - Apparatus for Oscillating Tests

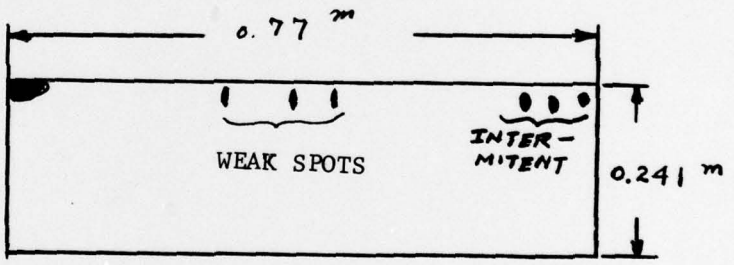

Figure 3a - P_{amb} = 76.6 KPa

Figure 3b - P_{amb} = 76.3 KPa

Figure 3 - Steady Flow Observation α = 3.5 deg.

FIGURE 4A INCEPTION OF CAVITATION (STEADY)

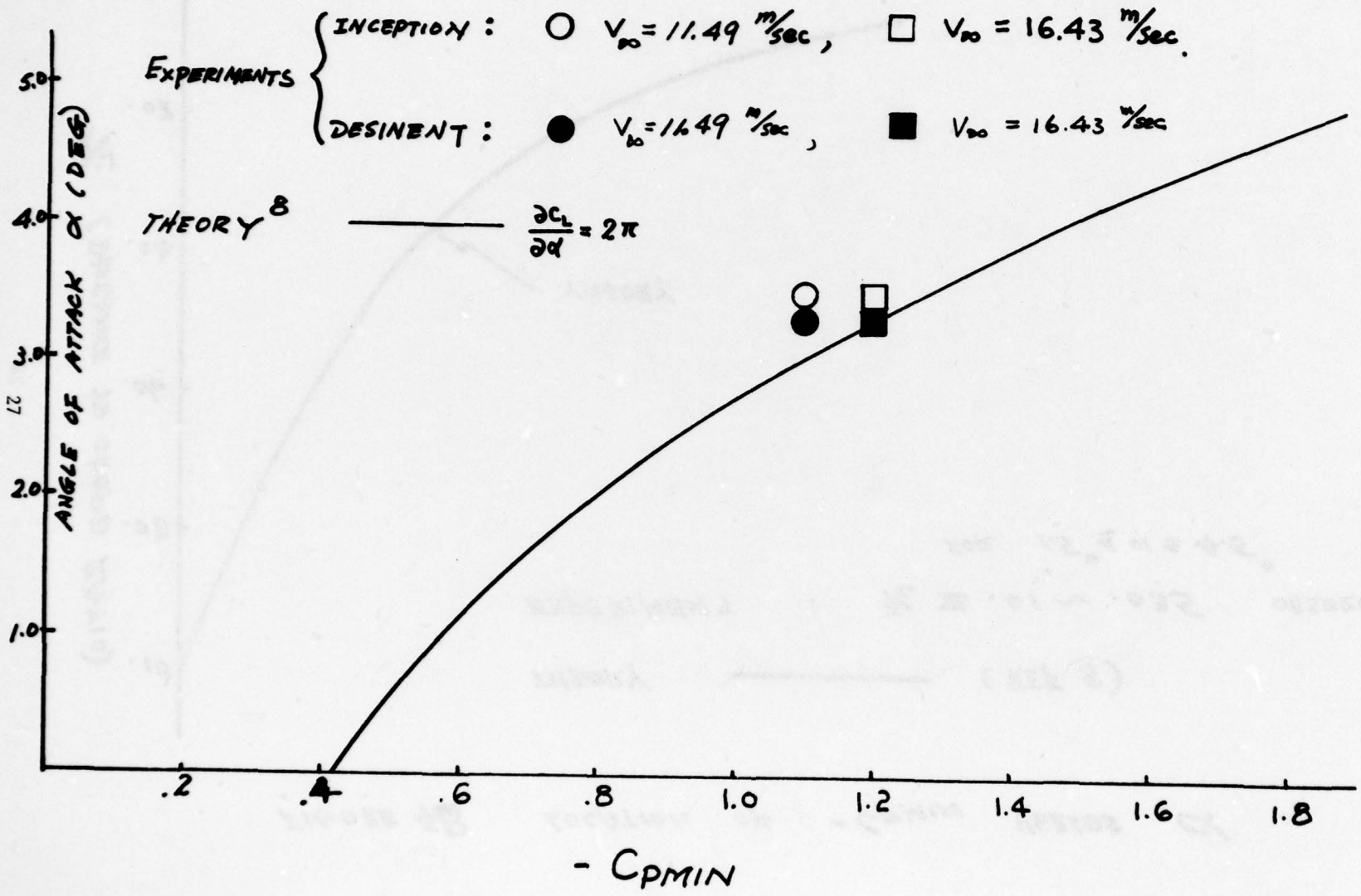

FIGURE 4B LOCATION OF $-C_{p_{MIN}}$ VERSUS α

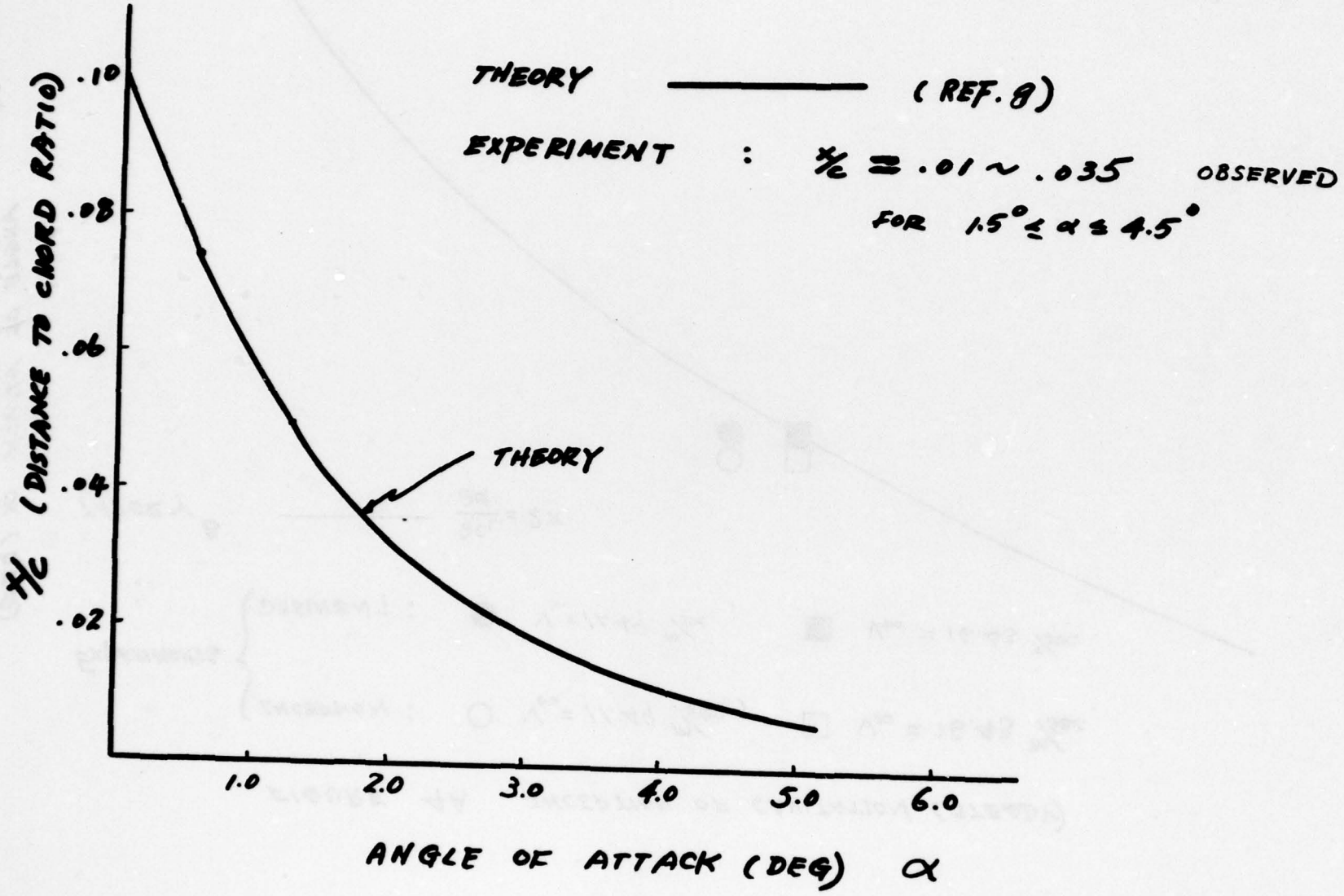

FIGURE 5 A TYPICAL HISTORICAL DIAGRAM OF α AND CAMERA PULSE SIGNAL

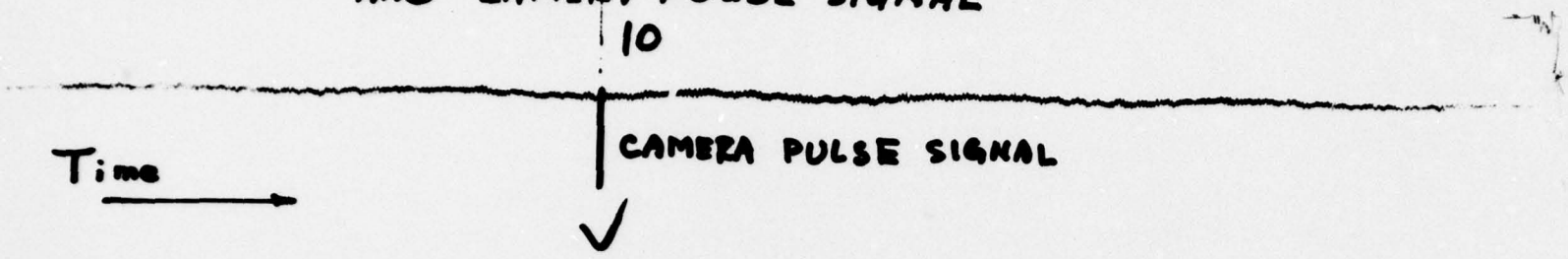

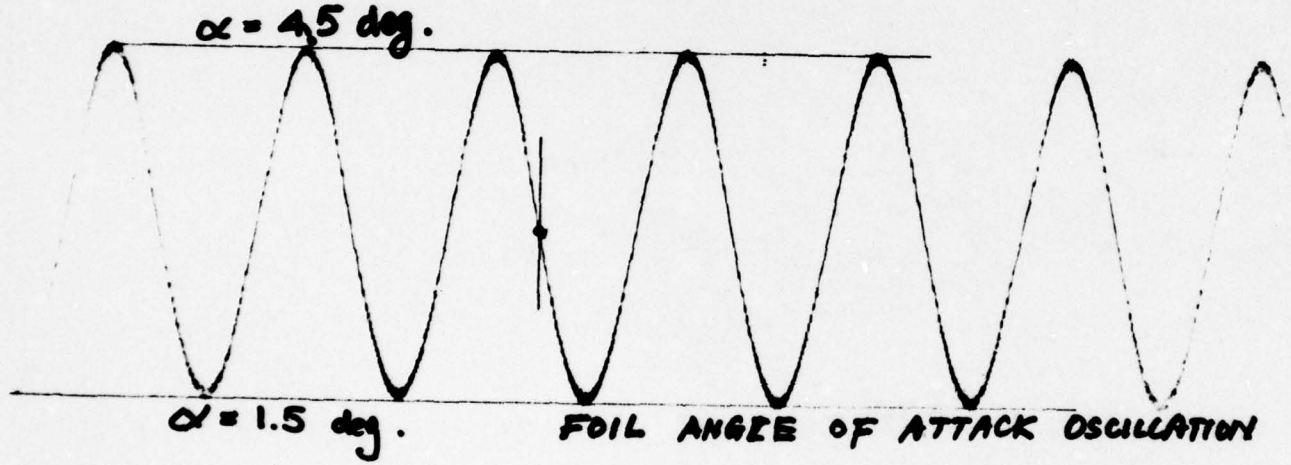

FIGURE 6 SEQUENTIAL FRAMES OF OSCILLATING TESTS
SERIES /30/ $\omega = 4.0$ HZ, $\bar{\alpha} = 1.0$ DEG.

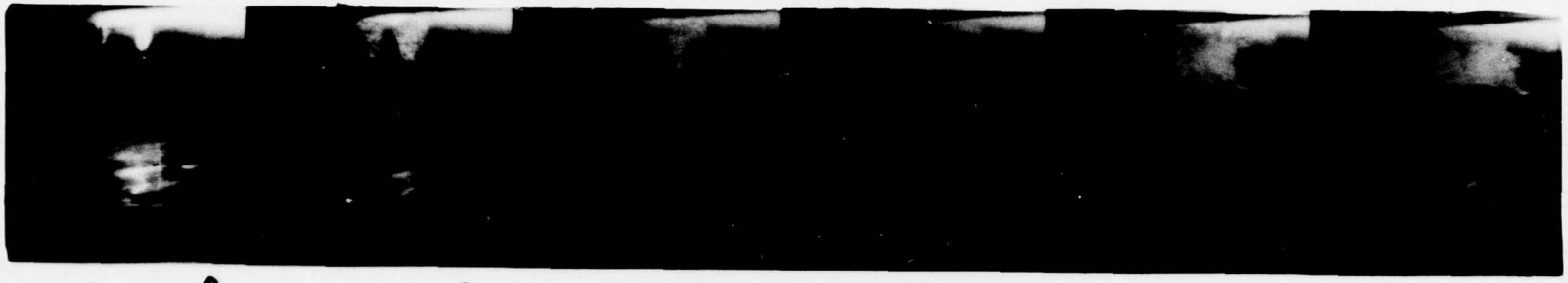

$\alpha = 3.74^\circ$ 3.88° 3.97° 4.0° 3.96° 3.87°

$\alpha = 3.72^\circ$ 3.51° 3.30° 3.05° 2.80° 2.56°

FIGURE 7 SEQUENTIAL FRAMES OF OSCILLATING TESTS

SERIES 1401 ω = 4.0 HZ, $\bar{\alpha}$ = 1.5 DEG

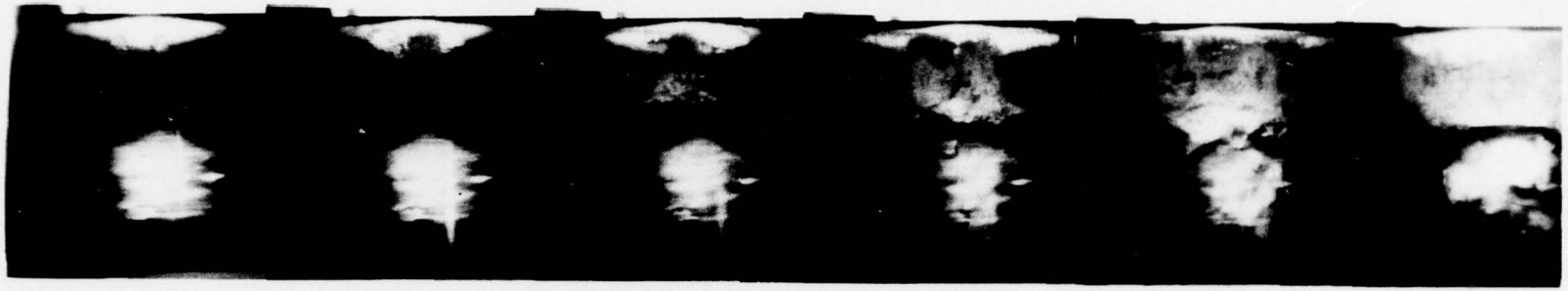

α = 4.11° 4.33° 4.46° 4.50° 4.45° 4.30°

α = 4.08° 3.78° 3.44° 3.07° 2.70° 2.34°

FIGURE 8 SEQUENTIAL FRAMES OF OSCILLATING TESTS

SERIES 1403 $\omega = 7.5$ HZ, $\bar{\alpha} = 1.5$ DEG.

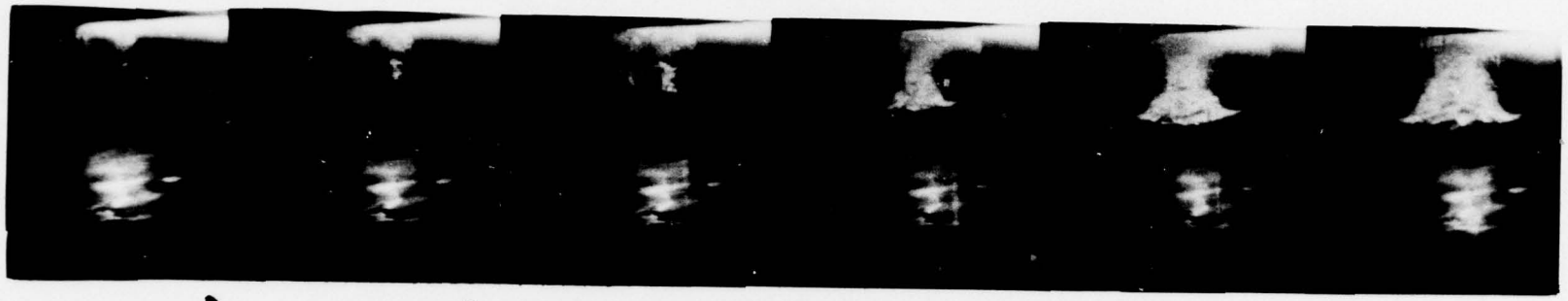

$\alpha = 4.11^\circ$ 4.33° 4.46° 4.50° 4.45° 4.30°

$\alpha = 4.08^\circ$ 3.78° 3.44° 3.07° 2.70° 2.34°

FIGURE 9 THEODORSEN'S UNSTEADY WING THEORY
PITCHING MOTION AROUND 1/4 CHORD

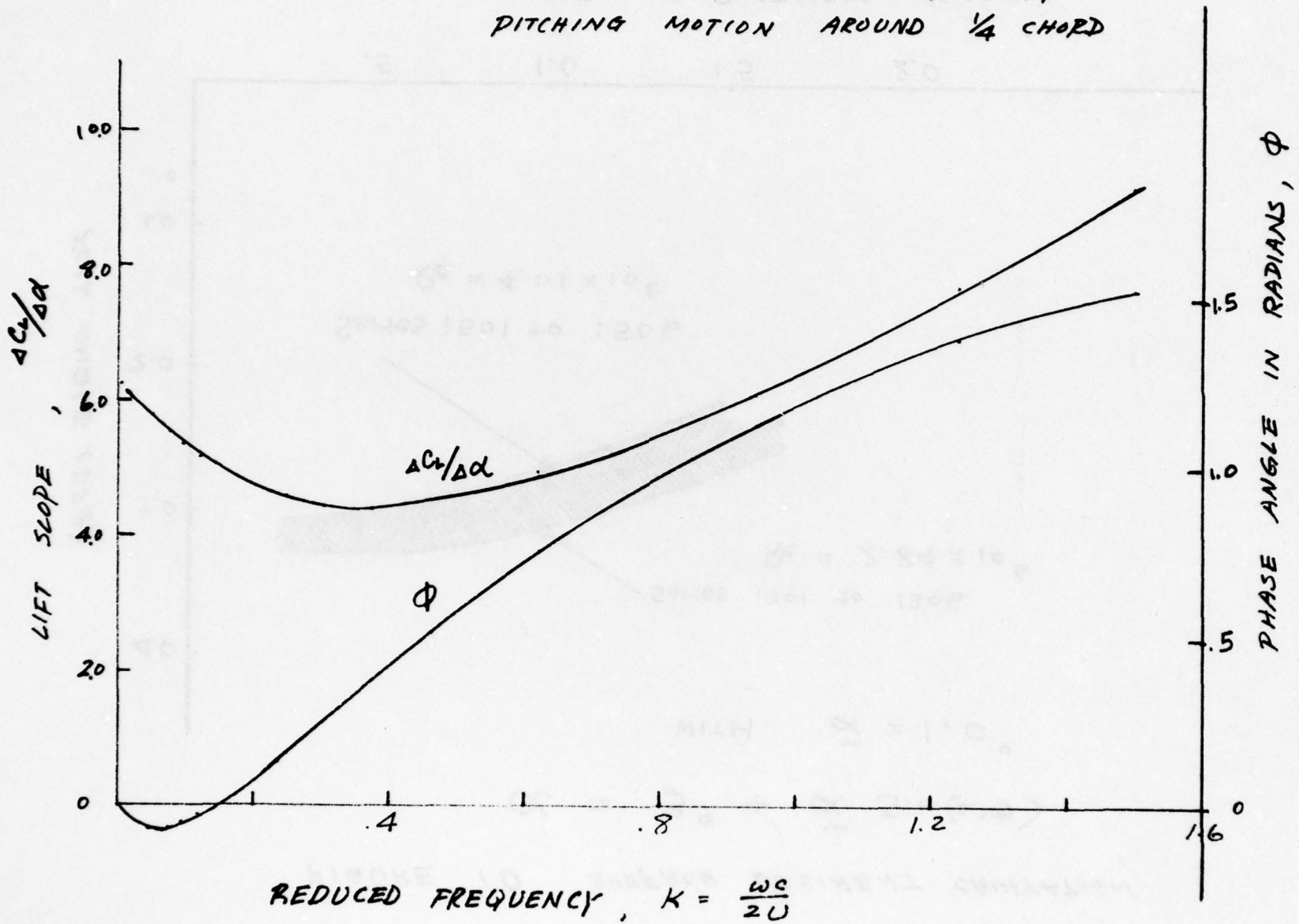

FIGURE 10 SURFACE DESINENT CAVITATION

$$\alpha = 3^\circ + \bar{\alpha} \sin(\omega t)$$

WITH $\bar{\alpha} = 1.0^\circ$

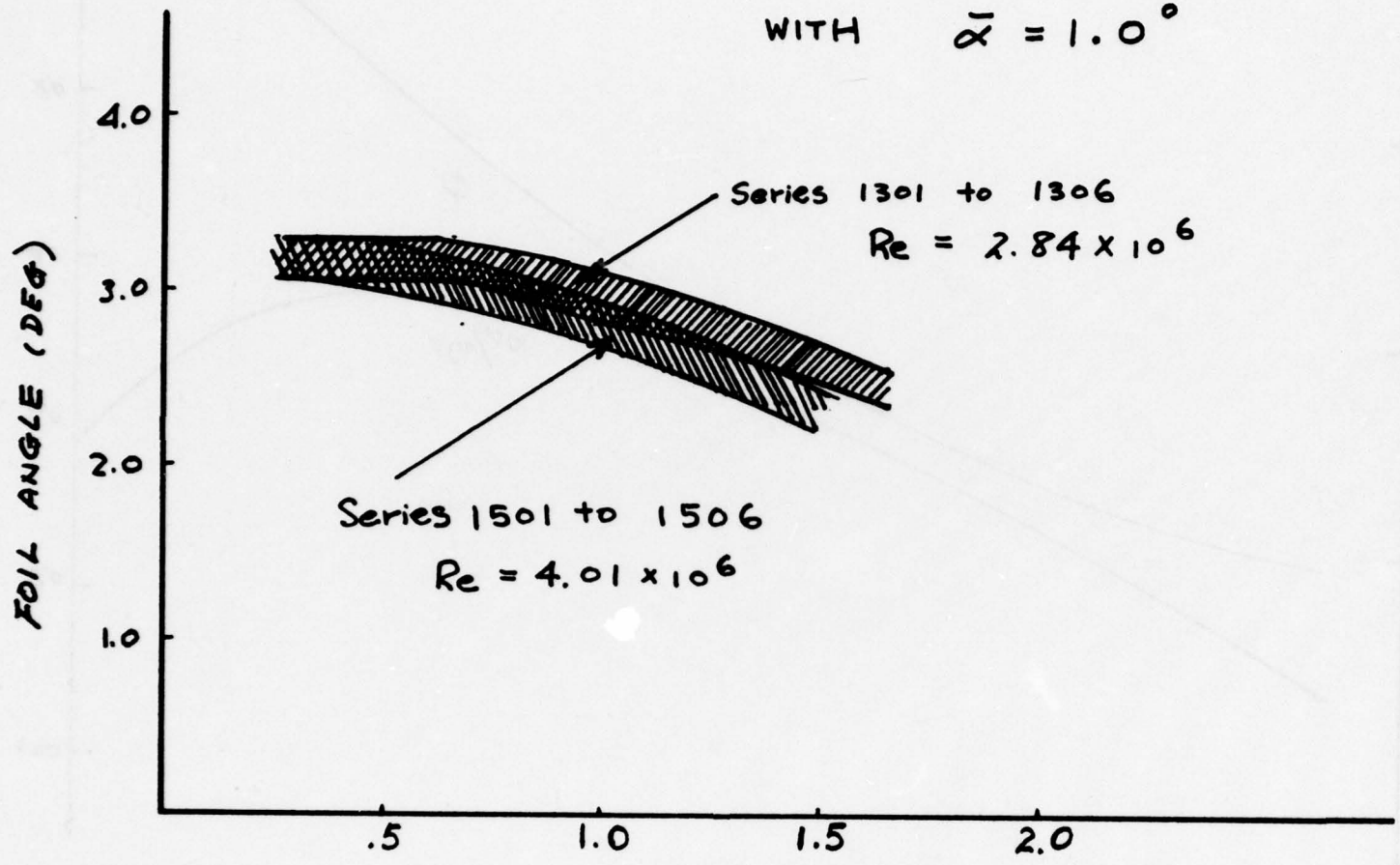

FIGURE 11 INFLUENCE OF PITCH AMPLITUDE ON SURFACE DESINENT CAVITATION

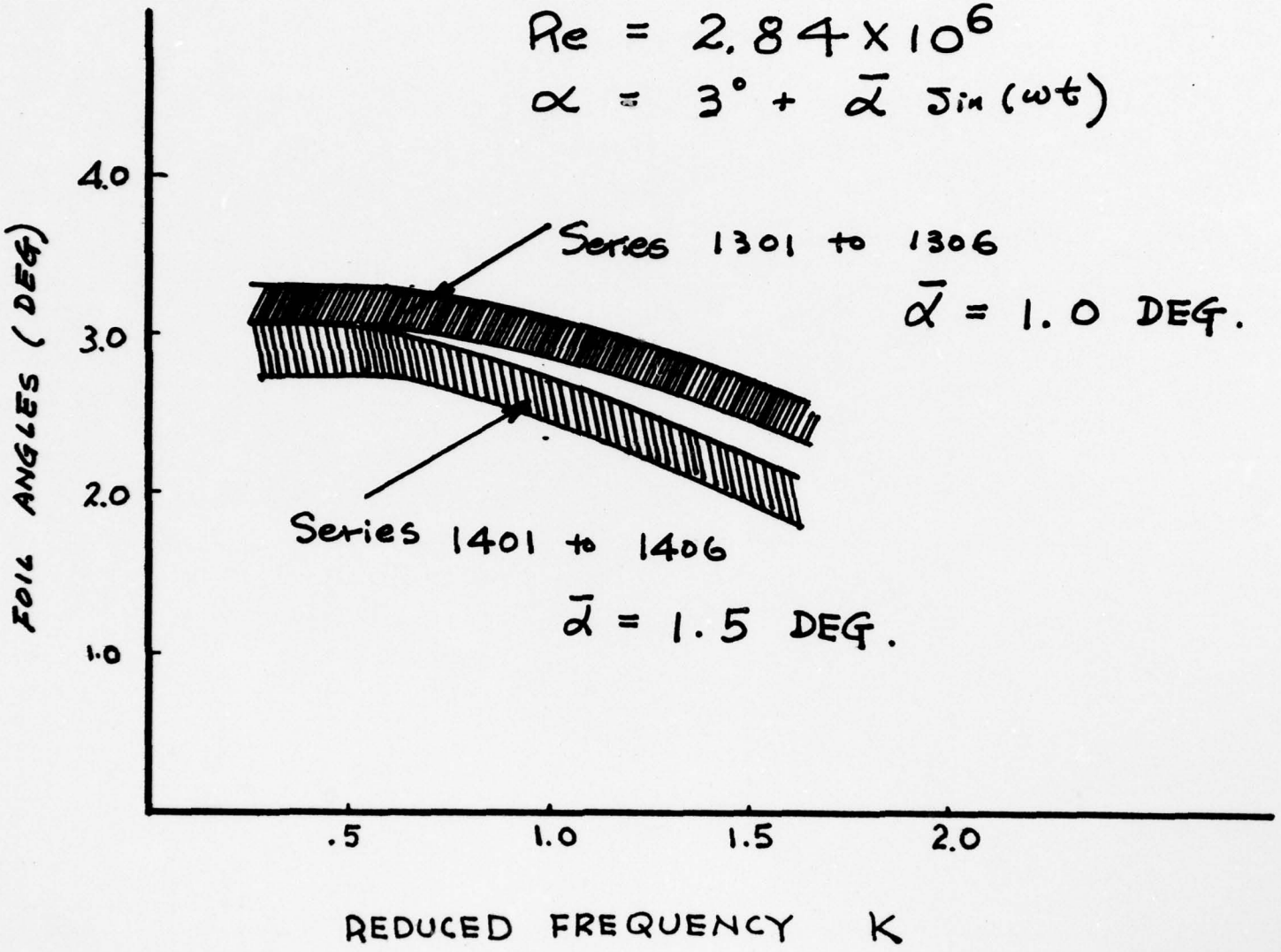

DTNSRDC ISSUES THREE TYPES OF REPORTS

1. DTNSRDC REPORTS, A FORMAL SERIES, CONTAIN INFORMATION OF PERMANENT TECHNICAL VALUE. THEY CARRY A CONSECUTIVE NUMERICAL IDENTIFICATION REGARDLESS OF THEIR CLASSIFICATION OR THE ORIGINATING DEPARTMENT.

2. DEPARTMENTAL REPORTS, A SEMIFORMAL SERIES, CONTAIN INFORMATION OF A PRELIMINARY, TEMPORARY, OR PROPRIETARY NATURE OR OF LIMITED INTEREST OR SIGNIFICANCE. THEY CARRY A DEPARTMENTAL ALPHANUMERICAL IDENTIFICATION.

3. TECHNICAL MEMORANDA, AN INFORMAL SERIES, CONTAIN TECHNICAL DOCUMENTATION OF LIMITED USE AND INTEREST. THEY ARE PRIMARILY WORKING PAPERS INTENDED FOR INTERNAL USE. THEY CARRY AN IDENTIFYING NUMBER WHICH INDICATES THEIR TYPE AND THE NUMERICAL CODE OF THE ORIGINATING DEPARTMENT. ANY DISTRIBUTION OUTSIDE DTNSRDC MUST BE APPROVED BY THE HEAD OF THE ORIGINATING DEPARTMENT ON A CASE-BY-CASE BASIS.